STEM CELLS®

TISSUE-SPECIFIC STEM CELLS

BM88/Cend1 Expression Levels Are Critical for Proliferation and Differentiation of Subventricular Zone-Derived Neural Precursor Cells

LIDA KATSIMPARDI,[a] MARIA GAITANOU,[a] CECILE E. MALNOU,[b] PIERRE-MARIE LLEDO,[c] PIERRE CHARNEAU,[b] REBECCA MATSAS,[a] DIMITRA THOMAIDOU[a]

[a]Laboratory of Cellular and Molecular Neurobiology, Hellenic Pasteur Institute, Athens, Greece; [b]Group of Molecular Virology and Vectorology, Institut Pasteur Paris, Paris, France; [c]Laboratory for Perception and Memory, Institut Pasteur Paris, Centre National de la Recherche Scientifique Unité de Recherche Associée 2182, Paris, France

Key Words. Adult neurogenesis • Neurospheres • Lentiviral vectors • RNA interference • Subventricular zone explants

ABSTRACT

Neural stem cells remain in two areas of the adult mammalian brain, the subventricular zone (SVZ) and the dentate gyrus of the hippocampus. Ongoing neurogenesis via the SVZ-rostral migratory stream pathway maintains neuronal replacement in the olfactory bulb (OB) throughout life. The mechanisms determining how neurogenesis is restricted to only a few regions in the adult, in contrast to its more widespread location during embryogenesis, largely depend on controlling the balance between precursor cell proliferation and differentiation. BM88/Cend1 is a neuronal lineage-specific regulator implicated in cell cycle exit and differentiation of precursor cells in the embryonic neural tube. Here we investigated its role in postnatal neurogenesis. Study of in vivo BM88/Cend1 distribution revealed that it is expressed in low levels in neuronal precursors of the adult SVZ and in high levels in postmitotic OB interneurons. To assess the functional significance of BM88/Cend1 in neuronal lineage progression postnatally, we challenged its expression levels by gain- and loss-of-function approaches using lentiviral gene transfer in SVZ-derived neurospheres. We found that BM88/Cend1 overexpression decreases proliferation and favors neuronal differentiation, whereas its downregulation using new-generation RNA interference vectors yields an opposite phenotype. Our results demonstrate that BM88/Cend1 participates in cell cycle control and neuronal differentiation mechanisms during neonatal SVZ neurogenesis and becomes crucial for the transition from neuroblasts to mature neurons when reaching high levels. STEM CELLS *2008;26:1796–1807*

Disclosure of potential conflicts of interest is found at the end of this article.

INTRODUCTION

In adult mammals, neurogenesis occurs within two discrete brain regions, the dentate gyrus of the hippocampus and the subventricular zone (SVZ) [1]; the process is sustained by the life-long persistence of neural stem cells (NSCs) in these two areas. Recent progress shows that neurons suitable for transplantation can be generated from adult NSCs maintained in culture but also that the adult brain itself produces new cells that differentiate into functional neurons in diseased areas [2, 3]. These findings raise hopes for the development of cell replacement therapies in neurodegenerative disorders, but they require a thorough understanding of the mechanisms regulating NSC proliferation and differentiation. The SVZ is the richest source of NSCs in the adult central nervous system (CNS), providing a continuous supply of neuroblasts to the olfactory bulb (OB), one of the few structures remaining active in the adult forebrain [4, 5]. In this area, the source of permanent cell production consists of multipotent NSCs belonging to the astroglial lineage [5]. These, called type B cells, are slowly dividing astrocytes that generate committed neuronal precursors (type A cells), passing through an intermediate type of rapidly dividing cells (transit-amplifying type C cells) [5]. An increasing number of molecules characterizing and/or participating in this B-C-A transition and cell fate restriction have been identified [6, 7]. However, the mechanisms, as well as the intrinsic and extrinsic factors governing the proliferation/differentiation characteristics of progenitor cells within the SVZ niche, are still under active investigation.

We have previously reported the neuronal protein BM88/Cend1 (hereafter designated Cend1 [cell cycle exit and neuronal differentiation 1]; National Center for Biotechnology Information nomenclature; http://www.ncbi.nih.gov) as a marker for cells committed to the neuronal lineage during primary neurogenesis [8, 9]. Cend1 is an integral membrane protein, anchored to the membrane of intracellular organelles, including the mitochondria and endoplasmic reticulum, via a transmembrane domain, with the bulk of the protein facing the cytoplasm [10,

Author contributions: L.K.: conception and design, collection and/or assembly of data, data analysis and interpretation; M.G.: collection and/or assembly of data, data analysis and interpretation; C.M.: collection and/or assembly of data; P.-M.L.: provision of study material, data analysis and interpretation; P.C.: provision of study material; R.M. and D.T.: conception and design, financial support, data analysis and interpretation, manuscript writing.

Correspondence: Dimitra Thomaidou, Ph.D., Laboratory of Cellular and Molecular Neurobiology, Hellenic Pasteur Institute, 127 Vassilissis Sofias Avenue, Athens 115 21, Greece. Telephone: 30-210-64-78-833; Fax: 30-210-64-78-833; e-mail: thomaidou@pasteur.gr Received November 2, 2007; accepted for publication May 13, 2008; first published online in STEM CELLS *EXPRESS* May 22, 2008. 1066-5099/2008/$30.00/0 doi: 10.1634/stemcells.2007-0921

11]. During embryonic development, Cend1 is expressed by neuroepithelial progenitors and radial glia when they generate neurons, whereas it is downregulated during gliogenesis. Of interest, Cend1 expression is elevated in differentiated neurons and decreased in mutants with neurogenesis defects [8], indicating its potential involvement in progenitor cell progression toward neuronal differentiation. In support of this, Cend1 is sufficient and necessary to drive neuroblastoma cells to cell cycle exit during G1 phase, by acting on the p53-cyclin D1-pRb signaling pathway, while directing them toward a neuronal phenotype [12]. Most importantly, Cend1 is involved in mechanisms coupling cell cycle exit and differentiation of neuronal precursors in the embryonic neural tube [13]. The intriguing observation that Cend1 is expressed in the adult SVZ [8] prompted us to investigate the specific cell types in which it is present along the SVZ-rostral migratory stream (RMS)-OB pathway and examine the effects of challenging its levels on cell cycle control and neuronal differentiation of SVZ-derived neurospheres.

MATERIALS AND METHODS

Construction and Production of Cend1-Expressing Lentiviral Vector

The coding region of the porcine Cend1 cDNA [11] was cloned into the unique BsiWI and BssHII sites of the pTRIP ΔU3 cytomegalovirus (CMV) plasmid to acquire pTRIP.ΔU3.CMV.Cend1 (pTrip.Cend1) plasmid, driving Cend1 expression under the control of the CMV early promoter. Vector particles (Fig. 3A, Trip.Cend1) were produced by transient calcium phosphate cotransfection of 293T cells with pTRIP.Cend1, the encapsidation plasmid (p8.7) [14], and the vesicular stomatitis virus G (VSV-G) envelope expression plasmid pHCMVG [15], as previously described [16]. Quantification of the p24 antigen content of vector particles was performed with a commercial HIV-1 p24 enzyme-linked immunosorbent assay kit (PerkinElmer Life and Analytical Sciences, Boston, http://www.perkinelmer.com).

Construction of Novel Short Hairpin RNA Vectors Targeting Cend1 mRNA

Construction of the pTripSym vector for expression of the Cend1 short hairpin RNA (shRNA) was performed by initially introducing restriction sites into the U3 part of the long terminal repeat (LTR) to allow further cloning of shRNA units. The ΔU3PL fragment of the pTrip-CMV-green fluorescent protein (GFP)-ΔU3PL plasmid was cloned into the pCR 2.1 TOPO vector (Stratagene, La Jolla, CA, http://www.stratagene.com). The KpnI/KpnI and XbaI/XbaI fragments were then removed, resulting in the pLTR-ΔU3PL plasmid with unique KpnI and XbaI restriction sites. A prehybridized oligonucleotide duplex with sense sequence 5′-ACG CGT ATC-GAT TGG CCA GCT AGC GTC GAC-3′ was then ligated into pLTR-ΔU3PL to introduce a polylinker containing a single NheI restriction site, which was then used to introduce the shRNA units. The KpnI/XbaI restriction fragment of this plasmid was transferred into the pTrip-CMV-GFP vectors to produce pTrip.CMV.GFP.ΔU3-polylinker plasmid. The minimal internal part of pTripSym was engineered as follows: three polymerase chain reactions (PCRs) were carried out using the pTrip.CMV.GFP.ΔU3-polylinker as matrix. Fragments amplified were as follows: the Ψ encapsidation fragment sense primer, 5′-AGG CGC CCG AAC AGG-3′; antisense primer, 5′-TTT GTC AAT AGA GGG TTG CTA C-3′; the Flap fragment sense primer, 5′-CCC TCT ATT GAC AAA GGC AGT ATT CAT CCA C-3′; antisense primer, 5′-GTG GGT GCT ACC AAA GTG GAT CTC TGC T-3′; and the RTA-responsive elements (RRE) fragment sense primer, 5′-TTT GGT AGC ACC CAC CAA GG-3′; antisense primer, 5′-TTG GTA CCC TAG CAT TCC AAG GCA C-3′. The Ψ-Flap-*RRE* fragment, which was obtained by a second round of PCR performed with the three PCR fragments together as matrix, was then cloned into the pCR 2.1 TOPO vector, and the BssHII/KpnI restriction fragment was then cloned into the pTrip.CMV.GFP.ΔU3-polylinker, resulting in the pTripSym.ΔU3-polylinker vector. The last step was to introduce the shRNA unit into pTripSym.ΔU3-polylinker, by linearizing the vector with NheI and ligating it with the Cend1 shRNA unit (Fig. 3B). This unit was obtained from pSuper-shRNACend1 by XbaI and SpeI digestion, to give the pLTR.ΔU3.shRNACend1 plasmid. Cend1 shRNA (OligoEngine, Seattle, WA, http://www.oligoengine.com) was constructed using the Cend1 siRNA sequence with the highest efficiency in silencing Cend1, as previously reported [12]. The sequence of Cend1-specific shRNA is available upon request. Vector particles for Trip.shCend1 were produced as described above. The same strategy was used for construction and production of the Trip.shLuc vector, targeting the Luciferase mRNA.

Neurosphere Cultures

All animals were handled according to European Union legislation for animals' rights (86/906/EEC). Neurosphere cultures were prepared as previously described [17] from the SVZ area of postnatal day 5 C57/BL6J mice. After 7 days in culture, floating neurospheres were trypsin-dissociated and allowed to re-form spheres at least three times before further use. Proliferation studies were performed either on free-floating neurospheres or after dissociation to single cells, plating onto poly-L-lysine coated coverslips, and further culture for 3 days in the presence of epidermal growth factor (EGF)/basic fibroblast growth factor (bFGF). For differentiation, whole-mount or dissociated neurospheres were plated on poly-L-lysine-coated coverslips and maintained for 3 days in the absence of growth factors. For Cend1 overexpression, cells were infected with the Trip.Cend1 or control Trip.GFP vectors at a final concentration of 260 ng/ml, at either the single-cell or whole-neurosphere stage. For Cend1 silencing, neurospheres were transduced with 300 ng/ml Trip.shCend1 or control Trip.shLuc lentiviral vectors. Cells were incubated with the lentiviral vectors for 6 hours, and transduction efficiency was estimated after 3 days by monitoring transgene or endogenous Cend1 expression.

Acute SVZ Cultures

Acute cultures were prepared from the SVZ area of adult C57/BL6J mice, following the same dissociation protocol as for neurosphere cultures. Dissociated cells were plated as 50-μl drops onto poly-L-lysine-coated coverslips and cultured for 3 hours before fixation.

SVZ Explant Cultures

Detailed methods are presented in supplemental online Materials and Methods.

Site-Directed Mutagenesis

Site-directed mutagenesis of the putative E-box sequence present on the *Cend1* 346-base pair (bp) pGL(−283/+63) minimal promoter fragment was carried out using the forward primer 5′-CTG CCT CTG GCA GTC C**TT** GA**A** A**G**G ACT TGG ACC CCG CA-3′ and the reverse primer 5′-TGC GGG GTC CAA GTC C**TT** TC**A** A**G**G ACT GCC AGA GGC AG-3′ in combination with the QuickChange Site-Directed Mutagenesis kit (Stratagene) according to the manufacturer's instructions. The mutated plasmids were subjected to sequencing analysis to confirm the mutation.

Transient Transfections and Luciferase Assays

Transfection of Neuro 2a (N2A) cells (American Type Culture Collection, Manassas, VA, http://www.atcc.org) was performed by lipofection, as previously described [18]. Transfection of neurospheres was performed using the Amaxa nucleofector apparatus and kit (Amaxa AG, Cologne, Germany, http://www.amaxa.com) according to the manufacturer's instructions. For estimation of Cend1 mRNA levels upon Neurogenin-1 (Ngn1) overexpression, proliferating neurospheres were transfected with 2 μg of Ngn1 expression plasmid, which was a kind gift of Dr. H. Ohkubo [19]. The mRNA of neurosphere cells was extracted 48 hours after transfection as described in supplemental online Materials and Methods.

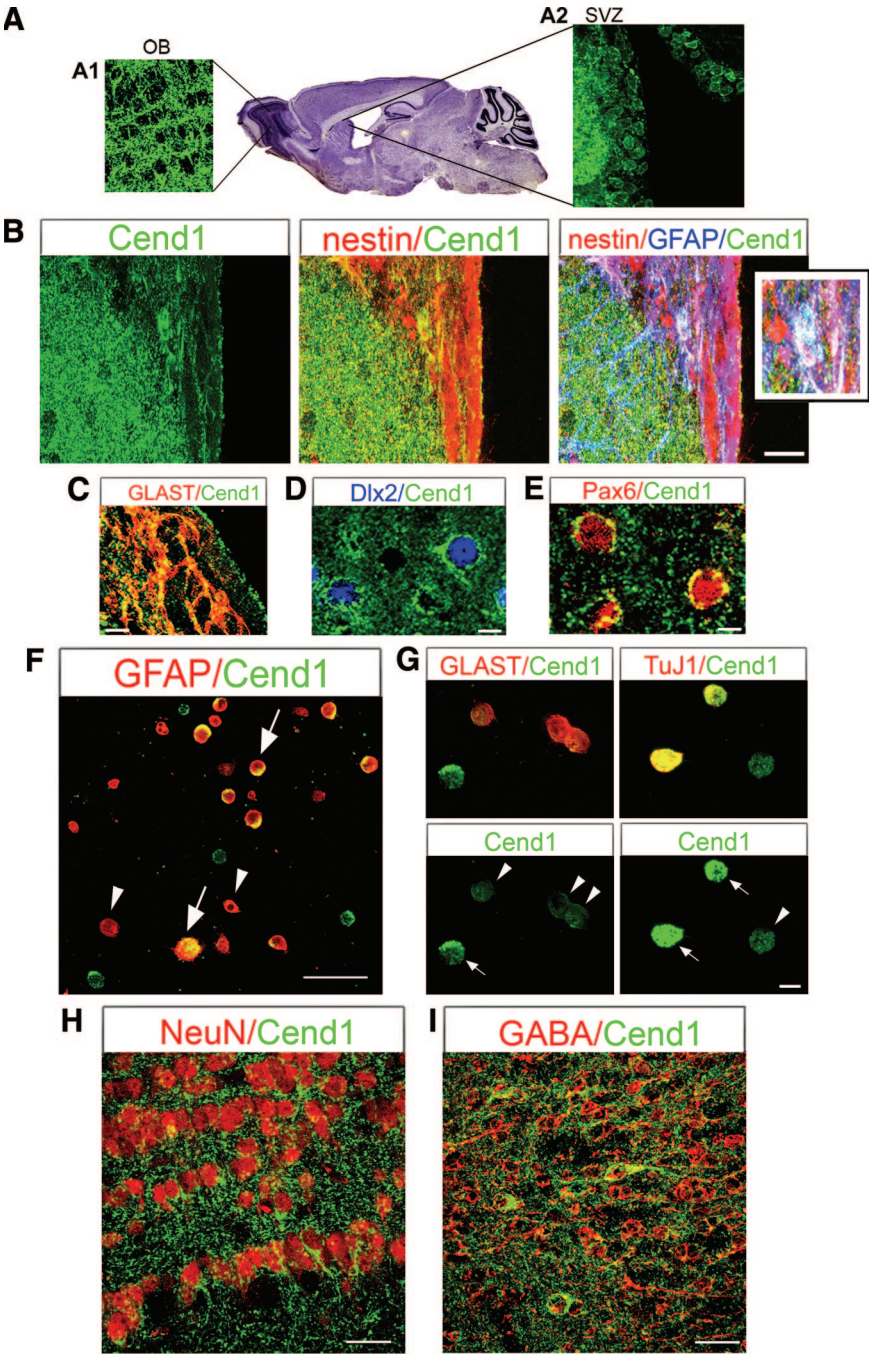

Figure 1. Expression of Cend1 in the adult SVZ and OB. **(A):** Nissl-staining of a sagittal section of adult mouse brain, including the region where the SVZ-rostral migratory stream (RMS)-OB pathway localizes. **(A1, A2):** Following immunofluorescence staining for Cend1 in higher magnification (insets), note the low but still detectable levels of Cend1 in the SVZ **(A2)** and high expression in differentiated granule neurons of the OB **(A1)**. **(B–F, H–I):** Maximum projections of confocal optical sections of the SVZ area and OB. **(B):** In the SVZ area, Cend1 is detected in the nestin$^+$/GFAP$^+$ NSC. The inset shows at higher magnification a triple-labeled Cend1$^+$/nestin$^+$/GFAP$^+$ cell. **(C):** Cend1 also colocalizes with the embryonic radial glia and adult NSC marker GLAST. **(D, E):** Double immunofluorescence labeling for Cend1 and Dlx2 indicates that both proteins colocalize in the SVZ area **(D)**, whereas double immunostaining of the anterior part of the SVZ and beginning of the RMS with antibodies to Cend1 and Pax6 indicate that Cend1 colocalizes with Pax6 **(E)**. **(F):** In acute cultures derived from adult SVZ, Cend1 colocalizes with a subpopulation of GFAP$^+$ cells (arrows). **(G):** In these acute cultures Cend1 expression levels (green) are lower in GLAST$^+$ cells (arrowheads, left panel) and significantly higher in βIII-tubulin$^+$ cells (arrows, right panel), appearing yellow from the merged green/red fluorescence of Cend1/βIII-tubulin colocalization. Quantification of Cend1 fluorescent intensity in individual cells, based on measurements from 50 independent cells for each condition, indicated that Cend1 expression is fivefold higher in differentiated neurons compared with precursor cells. **(H, I):** Coronal **(H)** and sagittal **(I)** sections of the OB depicting high expression of Cend1 in NeuN$^+$ neurons and in GABAergic interneurons (arrows). Scale bars = 20 μm **(A1, A2, B, G, H, I)**, 5 μm **(D, E)**, 10 μm **(C)**, and 40 μm **(F)**. Abbreviations: GFAP, glial fibrillary acidic protein; OB, olfactory bulb; SVZ, subventricular zone.

Transactivation experiments in both N2A cells and neurospheres, using either the wild-type or the E-box-mutated *Cend1* 346-bp pGL(−283/+63) minimal promoter fragment linked to the *Firefly* Luciferase gene, were performed as previously described [18], using a mixture containing 700 ng of pGL(−283/+63), 300 ng of a β-galactosidase expression plasmid (pCMVβ; Clontech, Palo Alto, CA, http://www.clontech.com), and 2 μg of Ngn1 expression plasmid. Luciferase activity was determined according to the manufacturer's instructions (Promega, Madison, WI, http://www.promega.com).

Immunohistochemistry, Reverse Transcription-PCR, and Western Blot Detection

Detailed methods are presented in supplemental online Materials and Methods.

RESULTS

Cend1 Is Expressed at Low Levels in Neural Stem/Progenitor Cells of the SVZ and at Higher Levels in Differentiated OB Neurons

Our initial immunohistochemical analysis revealed that along the adult mouse SVZ-RMS-OB pathway (Fig. 1A) Cend1 is expressed in low but detectable levels in the SVZ (Fig. 1A2), where proliferating neuronal precursors reside, and is elevated in areas of differentiated neurons, such as the OB (Fig. 1A1). To determine the cell type(s) expressing Cend1 in the SVZ, we performed double and triple labeling for Cend1 and characteristic markers of SVZ subtypes. To assess Cend1 expression in

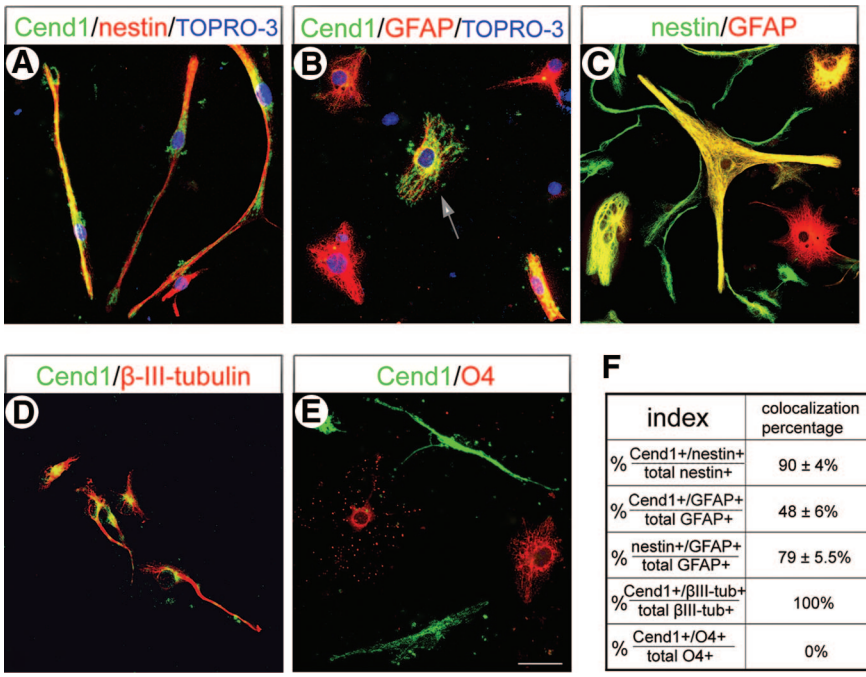

F

index	colocalization percentage
% Cend1+/nestin+ / total nestin+	90 ± 4%
% Cend1+/GFAP+ / total GFAP+	48 ± 6%
% nestin+/GFAP+ / total GFAP+	79 ± 5.5%
% Cend1+/βIII-tub+ / total βIII-tub+	100%
% Cend1+/O4+ / total O4+	0%

Figure 2. Immunofluorescence analysis of Cend1 expression in neurosphere cultures. Dissociated neurospheres were plated as single cells and cultured either in the presence **(A)** or in the absence **(B–E)** of epithelial growth factor and basic fibroblast growth factor. Shown are confocal images of cells stained for Cend1 and nestin **(A)**, Cend1 and GFAP **(B)**, nestin and GFAP **(C)**, Cend1 and βIII-tubulin with the TuJ1 antibody **(D)**, and Cend1 and O4 **(E)**. TOPRO-3 was used for nuclear staining **(A, B)**. Note that Cend1 is present in cells of the neuronal lineage **(A, D)**, as well as in a subpopulation of GFAP$^+$ cells **(B)**. **(F):** Table indicating colocalization percentages of Cend1 and the principal lineage markers, as well as the percentage of nestin$^+$ cells in the total GFAP$^+$ population. Scale bar = 20 μm. Abbreviation: GFAP, glial fibrillary acidic protein.

the type B cell population [20], we performed triple immunofluorescence labeling for Cend1, nestin, and glial fibrillary acidic protein (GFAP) (Fig. 1B). Numerous triple-labeled Cend1$^+$/nestin$^+$/GFAP$^+$ cells were detected within the SVZ neurogenic niche (Fig. 1B, main panel and inset). In contrast to its colocalization with GFAP in the SVZ (Fig. 1B), Cend1 did not colocalize with GFAP$^+$ astrocytes outside the SVZ area (data not shown; [8, 9]). Cend1 was also localized in (glutamate transporter) (GLAST$^+$) cells lying near the ventricle (Fig. 1C). These cells, which express the radial glial marker GLAST, have previously been shown to coincide with the GFAP$^+$ type B cell population of the SVZ [6, 21, 22]. To verify Cend1 expression in type B cells, as well as to quantify the extent of Cend1 localization in the GFAP$^+$ cell population, we performed double immunofluorescence labeling in dissociated cells derived from adult SVZ, 3 hours after plating (Fig. 1F). Double labeling for Cend1 and GFAP demonstrated that Cend1 is detected in 56.0% ± 2.8% of GFAP$^+$ cells of the SVZ at this age (Fig. 1F, arrows). Apart from its expression in type B cells, Cend1 is also present in Dlx2$^+$ transit-amplifying type C cells (Fig. 1D) and in Pax6$^+$ cells (Fig. 1E), which largely represent type A neuroblasts, but also some type C precursors [8].

In the OB Cend1 is expressed in mature NeuN$^+$ neurons (Fig. 1H) and in GABAergic local interneurons (Fig. 1I). In accordance with previous observations [8, 9], the levels of Cend1 expression are higher in brain regions where differentiated neurons lie (for example, in Fig. 1A, 1B, compare the low expression of Cend1 in the SVZ with the immediately adjacent area, where Cend1 is highly expressed). This observation was further verified by double immunocytochemical staining of adult SVZ acute cultures (Fig. 1G), with antibodies to Cend1 (Fig. 1G, lower panel) and markers of either precursor cells, such as GLAST, or differentiated neurons, such as βIII-tubulin. Quantification of Cend1 fluorescence intensity in individual cells using the Cell-R software (Olympus, Tokyo, http://www.olympus-global.com) confirmed that Cend1 expression levels were, on average, fivefold higher in βIII-tubulin$^+$ neurons compared with GLAST$^+$ precursor cells. Thus, the expression pattern of Cend1 indicates that it marks both neuronal progenitors and differentiated neurons and that a positive correlation links its expression levels to the degree of neuronal maturation.

Cend1 Attenuates Proliferation of Neonatal SVZ Neural Precursors

To investigate whether Cend1 expression has functional significance for neuronal lineage progression during secondary neurogenesis, we used neurosphere cultures [1, 23] derived from postnatal day 5 (P5) SVZ as a model system to study neuronal precursor proliferation and differentiation. These cells self-renew when cultured in the presence of EGF/bFGF, either as free-floating neurospheres or after dissociation and plating as single cells, whereas they can differentiate into neurons, astrocytes, and oligodendrocytes upon growth factor withdrawal. Confocal analysis of dissociated neurosphere cells 2 days after plating showed that Cend1 is expressed by 90% ± 4% of nestin$^+$ cells under proliferating conditions (Fig. 2A, 2F), whereas under differentiating conditions it is present in all βIII-tubulin$^+$ neurons (Fig. 2D) but not in O4$^+$ oligodendrocytes (Fig. 2E). Interestingly, Cend1 is also expressed by 48% ± 6% of GFAP$^+$ cells after 2 days in culture in the absence of growth factors (Fig. 2B, arrow). Since a large percentage (approximately 80%) of GFAP$^+$ cells in these cultures are also positive for nestin (Fig. 2C, 2F), a protein known to be expressed by immature astrocytes, it appears that Cend1 may also be expressed by immature astrocytes in vitro.

To assess the contribution of Cend1 in neuronal lineage progression early postnatally, we genetically manipulated its expression in P5 SVZ-derived neurospheres, where Cend1 was either overexpressed or silenced using appropriate lentiviral vectors (Fig. 3). The protocol used for cell transduction with the lentiviral vectors is schematically presented in Figure 4A. Neurospheres were transduced as free-floating spheres but also, in one particular type of experiment, after dissociation to single cells that were then brought to clonal density and allowed to form spheres again (Fig. 4A). To study the effect of Cend1 overexpression, the Trip.Cend1 lentiviral vector, driving the expression of porcine Cend1 cDNA under the control of the CMV promoter, was used (Fig. 3A). The respective control

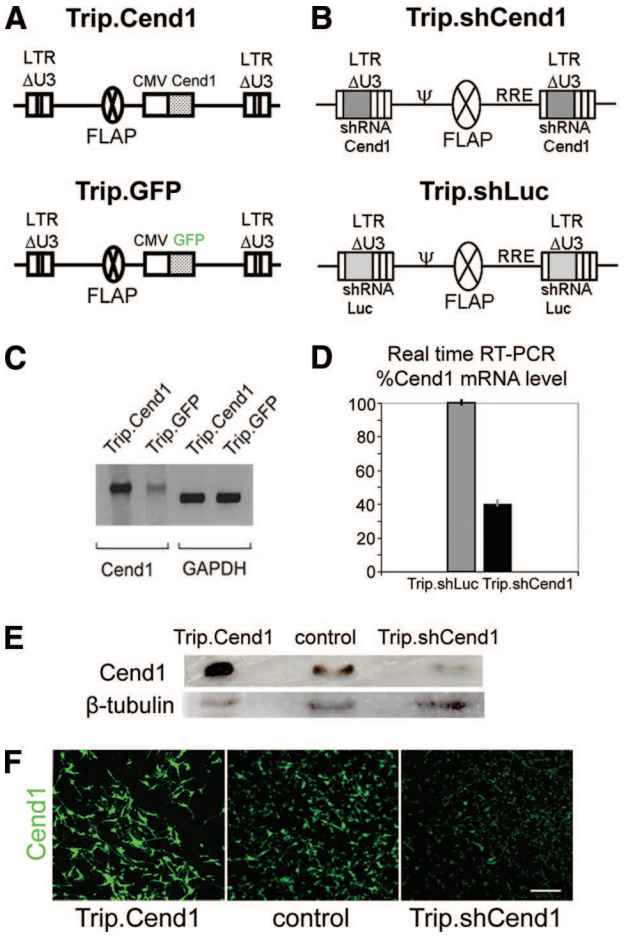

Figure 3. Lentiviral vectors used for manipulating the expression levels of Cend1. **(A):** Representation of the proviral form of the pTrip vectors coding for Cend1 (upper schema) and GFP (lower schema) under the CMV promoter. **(B):** Representation of the proviral form of the TripSym vectors encoding the shRNA targeting Cend1 (upper schema) or Luciferase (lower schema). The shRNA-expressing cassettes are inserted into the U3 part of the LTR, and the internal part of the vector contains only the Ψ and RRE elements, with the central DNA FLAP. **(C):** Transgene Cend1 mRNA expression in neurosphere cultures 4 days after transduction determined by semiquantitative RT-PCR. Note that transgene Cend1 is highly expressed in cultures transduced with Trip.Cend1 compared with cultures transduced with Trip.GFP. GAPDH expression serves as control for loaded mRNA. **(D):** Transduction of neurospheres with the Trip.shCend1 lentiviral vector and determination of endogenous Cend1 mRNA levels by real-time RT-PCR 4 days after transduction revealed a 60% ± 4% downregulation of Cend1 mRNA in Trip.shCend1-transduced neurosphere cultures compared with Trip.shLuc-transduced cultures. **(E):** Western blot analysis of Cend1 protein expression in control neurospheres, as well as in neurospheres transduced with Trip.Cend1 or Trip.shCend1. β-Tubulin was used for estimation of loaded protein and normalization of Cend1 levels. **(F):** Immunofluorescence labeling of dissociated neurospheres for Cend1 protein, 4 days following lentiviral transduction with either Trip.Cend1 or Trip.shCend1 viral vector, showing the corresponding increase and decrease in the number of Cend1-overexpressing or -expressing cells, compared with control (nontransduced) neurosphere cultures. Measurement of total fluorescence intensity of Cend1 expression levels in all three conditions using CellR̂ software (Olympus) indicated that upon Trip.Cend1 transduction, Cend1 levels rise 2.7 times compared with control, whereas following Trip.shCend1 transduction, Cend1 fluorescence has a twofold decrease compared with control. Abbreviations: CMV, cytomegalovirus; GAPDH, glyceraldehyde-3-phosphate dehydrogenase; GFP, green fluorescent protein; LTR, long terminal repeat; RT-PCR, reverse transcription-polymerase chain reaction; sh, short hairpin; RRE, RTA-responsive elements.

vector was Trip.GFP driving expression of the GFP protein (Fig. 3A). Silencing of Cend1 was achieved via the Trip.shCend1 lentiviral vector, whereas as control, a Trip.shLuc vector was used (Fig. 3B). Transgene Cend1 expression was verified by semiquantitative reverse transcription (RT)-PCR using primers specific for both porcine and mouse Cend1-mRNA (Fig. 3C). Quantification of the intensity of the produced mRNA and protein bands relative to glyceraldehyde-3-phosphate dehydrogenase and β-tubulin, respectively, revealed a 2.7-fold increase of Cend1 mRNA and 2.9-fold increase of Cend1 protein levels, in Trip.Cend1-transduced compared with Trip.GFP-transduced neurospheres (Fig. 3D, 3E). Conversely, Cend1 silencing was verified by both real-time RT-PCR and Western blot, which revealed a 60% ± 4% and 85% decrease of Cend1 mRNA and protein levels, respectively, in Trip.shCend1-transduced compared with Trip.shLuc-transduced neurospheres (Fig. 3D, 3E). In addition, immunofluorescence staining and counting of the number of cells in which Cend1 was either overexpressed or silenced revealed that the transduction efficiency of the Trip.Cend1 vector was 85% ± 5%, and transduction efficiency of the Trip.shCend1 silencing vector was 74% ± 4% (Fig. 3F). Transduction of neurospheres with the corresponding control viral vectors (Trip.GFP and Trip.shLuc) did not cause any change in Cend1 expression levels, compared with nontransduced cells (data not shown).

To determine the effect of Cend1 overexpression in cell proliferation, neurospheres were dissociated, lentivirally transduced at the single-cell level, and allowed to re-form floating spheres that were composed of progeny that also overexpressed Cend1. An important reduction in cell proliferation was observed in response to Cend1 overexpression (Fig. 4B–4D). Four days after transduction, neurospheres derived from Trip.Cend1-transduced cells had a statistically significant ($p < .05$) 2.5-fold reduction in sphere diameter compared with control neurospheres regrown from Trip.GFP-transduced cells (Fig. 4C, 4D). This size reduction was also obvious in secondary formed neurospheres overexpressing Cend1; however, no apparent changes were noted in the total number of secondary spheres generated (supplemental online Fig. 1). However, transduction at the single-cell level with the silencing Trip.shCend1 lentiviral vector resulted in formation of almost double the number (1.7-fold increase) of secondary-formed neurospheres compared with control (supplemental online Fig. 1), suggesting that Cend1 affects both neurosphere size and the number of neurospheres formed.

To further investigate the effect of Cend1 in cell proliferation, we estimated the 5-bromo-2′-deoxyuridine (BrdU) incorporation rate of cells infected in the sphere stage and then plated as single cells under proliferative conditions for 72 hours prior to analysis. Cells were given a 2-hour BrdU pulse before fixation, and estimation of the BrdU incorporation index out of the total number of 4,6-diamidino-2-phenylindole $(DAPI)^+$ nuclei revealed a statistically significant reduction from 5.2% ± 0.5% in Trip.GFP-transduced cultures to 2.0% ± 0.6% in Trip.Cend1-transduced cultures ($p < .05$; Fig. 4E, 4F). No difference in apoptotic cell death was observed between Trip.Cend1-transduced and Trip.GFP cells as estimated by activated caspase-3 staining (Fig. 4H, 4I). These findings suggest that elevation of Cend1 expression induces a significant subpopulation of neurosphere cells to exit from the cell cycle and/or proliferate at a slower pace because of cell cycle elongation. Thus, we explored the levels of Cyclin D1, a protein playing fundamental role in cell cycle progression control. Real-time RT-PCR measurements indicated a 67% ± 5% decrease of Cyclin D1 mRNA levels in Trip.Cend1-transduced compared with Trip.GFP-transduced cultures (Fig. 4G). Since the levels of cell cycle mediators are regulated to a great extent post-transcriptionally, we also

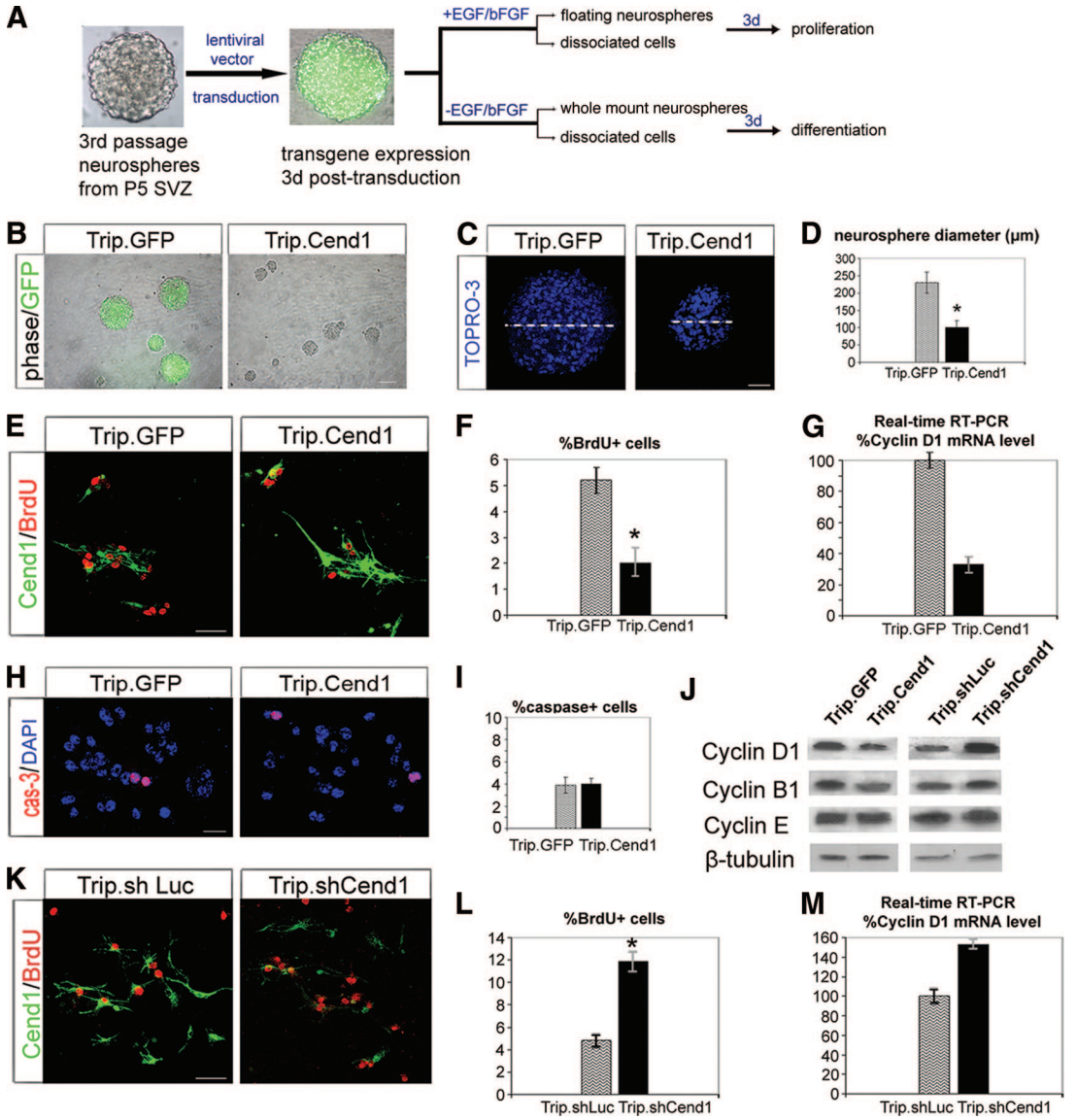

Figure 4. Effect of Cend1 overexpression and silencing on neurosphere proliferation. **(A):** Schematic representation of the experimental protocol used for neurosphere infection and culture. Third-passage postnatal day 5 SVZ neurospheres were transduced with Trip.Cend1 or the control Trip.GFP lentiviral vector. Three days after transduction, neurospheres were either left as free-floating spheres or dissociated to single cells and further grown for another 3 d, unless otherwise indicated, in the presence or absence of growth factors to assess proliferation or differentiation, respectively. The same strategy was used with the RNA interference set of lentiviral vectors, Trip.shCend1 and the control Trip.shLuc. **(B–D):** Effect of Cend1 overexpression on neurosphere size. Dissociated neurospheres were transduced and allowed to re-form floating spheres, and estimation of neurosphere size took place 4 d post-transduction. Note the smaller size of floating neurospheres upon Cend1 overexpression, compared with GFP-transduced ones, illustrated with fluorescence/phase contrast optics **(B)** and at a higher magnification with TOPRO-3 nuclear staining **(C)**. **(D):** Estimation of neurosphere diameter indicates a 2.5-fold reduction in size in response to Trip.Cend1, compared with Trip.GFP transduction. $*$, $p < .05$ ($n = 3$). **(E–J):** Effect of Cend1 overexpression on neurosphere cycling properties. **(E):** Upon forced expression of Cend1, dissociated neurospheres cultured under proliferative conditions exhibit reduced BrdU incorporation compared with Trip.GFP-transduced ones, as revealed by double immunofluorescence labeling. **(F):** Quantification of $BrdU^+$ cells following a 2-hour BrdU pulse in Cend1-overexpressing neurospheres, compared with control. Measurements were effectuated by dissociating the spheres and counting $BrdU^+$ cells out of total $DAPI^+$ nuclei. $*$, $p < .05$ ($n = 4$). **(G):** Real-time RT-PCR measurements indicate a 67% ± 5% reduction of Cyclin D1 mRNA levels upon Cend1 overexpression in neurosphere cultures. **(H, I):** Cend1 overexpression does not induce apoptosis, as indicated by immunohistochemistry for activated caspase-3 **(H)** and quantification of apoptotic profiles **(I)** that show 4% caspase-3^+ cells in both Trip.Cend1- and Trip.GFP-transduced neurosphere populations (4% ± 0.5% for Trip.Cend1 vs. 3.9 ± 0.7 for Trip.GFP-transduced cells). **(J):** Western blot analysis also reveals a decrease, predominantly in Cyclin D1, but also B1 levels upon Cend1 overexpression. **(J–M):** Effect of Cend1 knock-down on neurospheres' cycling properties. **(K):** Silencing of Cend1 by Trip.shCend1 transduction enhances proliferation compared with control Trip.shLuc transduction, as revealed by Cend1/BrdU double immunostaining. **(L):** Counting of $BrdU^+$ cells in Trip.shCend1-transduced versus control neurospheres indicates a 2.4-fold increase in BrdU incorporation (11.9% ± 0.8% BrdU index in Trip.sh.Cend1-transduced cultures vs. 4.8% ± 0.2% in Trip.shLuc-transduced cultures); $p < .05$ ($n = 5$). **(M):** Real-time RT-PCR measurements of Cyclin D1 mRNA in neurospheres transduced with Trip.shCend1 or Trip.shLuc showing a 53% ± 6.5% increase upon Cend1 knock-down. **(J):** Western blot analysis indicates elevated protein levels of Cyclin D1 and, to a lesser extent, B1 upon Cend1 silencing. Because of different total protein loading between the overexpression and silencing experiments, as revealed by β-tubulin levels, staining intensities for cycling protein bands are not comparable between the two control situations presented. Scale bars = 100 μm **(B)** and 40 μm **(C, E, H, K)**. Abbreviations: bFGF, basic fibroblast growth factor; BrdU, 5-bromo-2′-deoxyuridine; d, days; DAPI, 4,6-diamidino-2-phenylindole; EGF, epidermal growth factor; GFP, green fluorescent protein; RT-PCR, reverse transcription-polymerase chain reaction; sh, short hairpin; SVZ, subventricular zone.

estimated the protein levels of Cyclins D1, B1, and E in Cend1-transduced neurospheres by Western blot. In accordance, a reduction of the protein levels of Cyclin D1 and, to a smaller extent, of Cyclin B1 was evident, whereas the protein levels of Cyclin E were not apparently affected (Fig. 4J).

To verify Cend1 participation in cell cycle progression/exit of proliferating precursors, we performed RNA interference experiments, using the lentiviral vectors Trip.shCend1 and Trip.shLuc as control (Fig. 3B). Silencing of Cend1 in proliferating neurospheres followed by dissociation and plating under proliferative conditions resulted in a statistically significant 2.4-fold increase in BrdU incorporation (Fig. 4K, 4L). Cend1 silencing also caused a 53% ± 6.5% increase in Cyclin D1 mRNA (Fig. 4M) and protein (Fig. 4J) levels compared with Trip.shLuc-infected cultures, whereas the protein levels of Cyclin E were not affected (Fig. 4J). To ensure that the effect of Cend1 on cell cycle progression observed in dissociated cells was an instructive rather than a selective postdissociation process because of elimination of apoptotic cells, we performed clonal analysis on whole-mount neurospheres transduced with either the overexpressing or the silencing Cend1 lentiviral vectors. First, we checked for apoptotic cells by immunostaining for activated caspase-3 and found that in both cases apoptosis levels were identical to those of the respective control conditions (supplemental online Fig. 2A, 2C). Then we assessed proliferation using antibodies to phosphorylated histone-3 and Ki67 proteins (supplemental online Fig. 2B, 2C). Both gain- and loss-of-function approaches in whole-mount neurospheres concluded that Cend1 overexpression results in reduced proliferative capacity, whereas its downregulation yields the opposite effect (supplemental online Fig. 2B, 2C). Taken together these findings indicate that Cend1 forms part of the machinery controlling the cell cycle properties of postnatal SVZ-derived NSCs.

Cend1 Promotes Neuronal Differentiation of Neonatal SVZ-Derived Neuronal Precursors

Cell cycle progression and differentiation are two tightly linked cellular events. We therefore sought to investigate Cend1 implication in the differentiation program of SVZ-derived precursors. To this end, lentivirally transduced neurospheres derived from P5 SVZ, either overexpressing or downregulating Cend1, were analyzed in relation to their fate choice. Neurospheres were infected with the corresponding lentiviral vectors while in the free-floating stage, left for 3 days, and then cultured for another 3 days in the absence of growth factors, either as whole-mount preparations or as dissociated cells. Immunohistochemical staining of whole-mount differentiating neurospheres revealed that, qualitatively upon forced Cend1 expression, neuronal markers such as doublecortin and βIII-tubulin were highly upregulated, whereas astrocytic markers such as GFAP were downregulated compared with control spheres (Fig. 5A). To quantify the number of cells expressing these molecular markers in Cend1- and GFP-transduced cultures, neurospheres were dissociated to single cells and further cultured for 3 days. Analysis of immunocytochemically stained cells revealed a statistically significant 68.7% ± 4% increase in doublecortin$^+$ cells, a 100% ± 0.6% increase in βIII-tubulin$^+$ cells, and a 32% ± 5% decrease in GFAP$^+$ cells (Fig. 5B). There was no statistically significant decrease in O4 levels, suggesting that Cend1 is not involved in oligodendrocyte lineage progression (Fig. 5B). Accordingly, Cend1 knockdown had an opposite effect in the differentiation pathway of precursor cells (Fig. 5C). When Cend1 was silenced, neurospheres presented a less differentiated neuronal phenotype, as judged by the reduced expression of doublecortin and βIII-tubulin in whole-mount neurospheres (Fig. 5C). Quantification of this effect in dissociated neurospheres showed a statistically significant 44% ± 2.5% decrease in doublecortin$^+$ cells, a 45.4% ± 0.3% decrease in βIII-tubulin$^+$ neurons, and only a 13.9% ± 3.5% increase in GFAP-expressing astrocytes, whereas there was no statistically significant change in the percentages of O4$^+$ cells in Trip.shCend1-transduced compared with Trip.shLuc-transduced neurospheres (Fig. 5D). Consistently, an increase and a corresponding decrease in βIII-tubulin$^+$ neurons were estimated upon Cend1 overexpression and downregulation, respectively, when clonal analysis was performed in whole-mount neurospheres. Thus, Cend1 overexpression resulted in 26 ± 5 βIII-tubulin$^+$ cells per sphere, compared with 15 ± 2 βIII-tubulin$^+$ cells in control spheres and 8 ± 2 βIII-tubulin$^+$ cells in Trip.shCend1-transduced spheres (Fig. 5Ae, 5Af, 5Ce, 5Cf; supplemental online Fig. 3). Apoptosis levels were identical in all situations (data not shown).

To investigate whether Cend1 forms part of a cell cycle exit/neuronal differentiation pathway, we investigated whether its overexpression in neurosphere cultures results in changes in the expression levels of Notch1 and its downstream effector Hes1. Western blot analysis revealed that Cend1-transduced neurospheres exhibit lower protein amounts of both Notch1 and Hes1 compared with GFP-transduced neurospheres (Fig. 6A). We next asked whether endogenous Cend1 expression is regulated by transcription factors inducing neurogenesis, such as basic helix-loop-helix (bHLH) proneural genes. Of these, we chose to examine the effect of Ngn1, since this proneural gene has previously been shown to transactivate the minimal Cend1 promoter in neural cell lines in vitro [18]. In agreement, real-time RT-PCR measurements revealed that Ngn1 overexpression in the neurosphere system caused a 35% increase in Cend1 mRNA levels (Fig. 6B). To validate the Ngn1 effect on Cend1 expression levels, we checked the ability of Ngn1 to activate the Cend1 promoter directly. Computer-assisted analysis identified a consensus E-box sequence on the proximal Cend1 promoter, representing a putative bHLH protein binding site (Fig. 6C). Transactivation experiments were performed by cotransfecting the Ngn1 expression vector with either the E-box containing wild-type pGL(−283/+63) vector for expression of the 346-bp *Cend1* minimal promoter, or the same vector carrying four point mutations at the consensus E-box (Fig. 6C). Luciferase reporter assays in both the N2A neuroblastoma cell line and in neurosphere cultures demonstrated a threefold increase in wild-type Cend1 promoter activity upon Ngn1 overexpression, which is abolished following mutation of the E-box (Fig. 6D). This indicates that Cend1 forms part of the neuronal differentiation pathway activated by proneural genes in the adult.

Cend1 Affects Chain Formation in Explant Cultures Derived from Neonatal SVZ

To investigate whether the impact of Cend1 overexpression or silencing on cell cycle exit has also a potential effect on neuronal migration, we used P5 SVZ-explant cultures that mimic in vivo chain migration. Wild-type and Trip.GFP-transduced explants presented the normal pattern of chains migrating radially out of the explant, whereas following Trip.Cend1 lentiviral transduction, explants manifested a reduction in the number of chains migrating out of the explant core (Fig. 7A). Estimation of the number of DAPI$^+$ nuclei lying out of the explant core in Trip.GFP and Trip.Cend1-transduced explants revealed a statistically significant 45% ± 7% decrease in response to Cend1 compared with GFP (Fig.

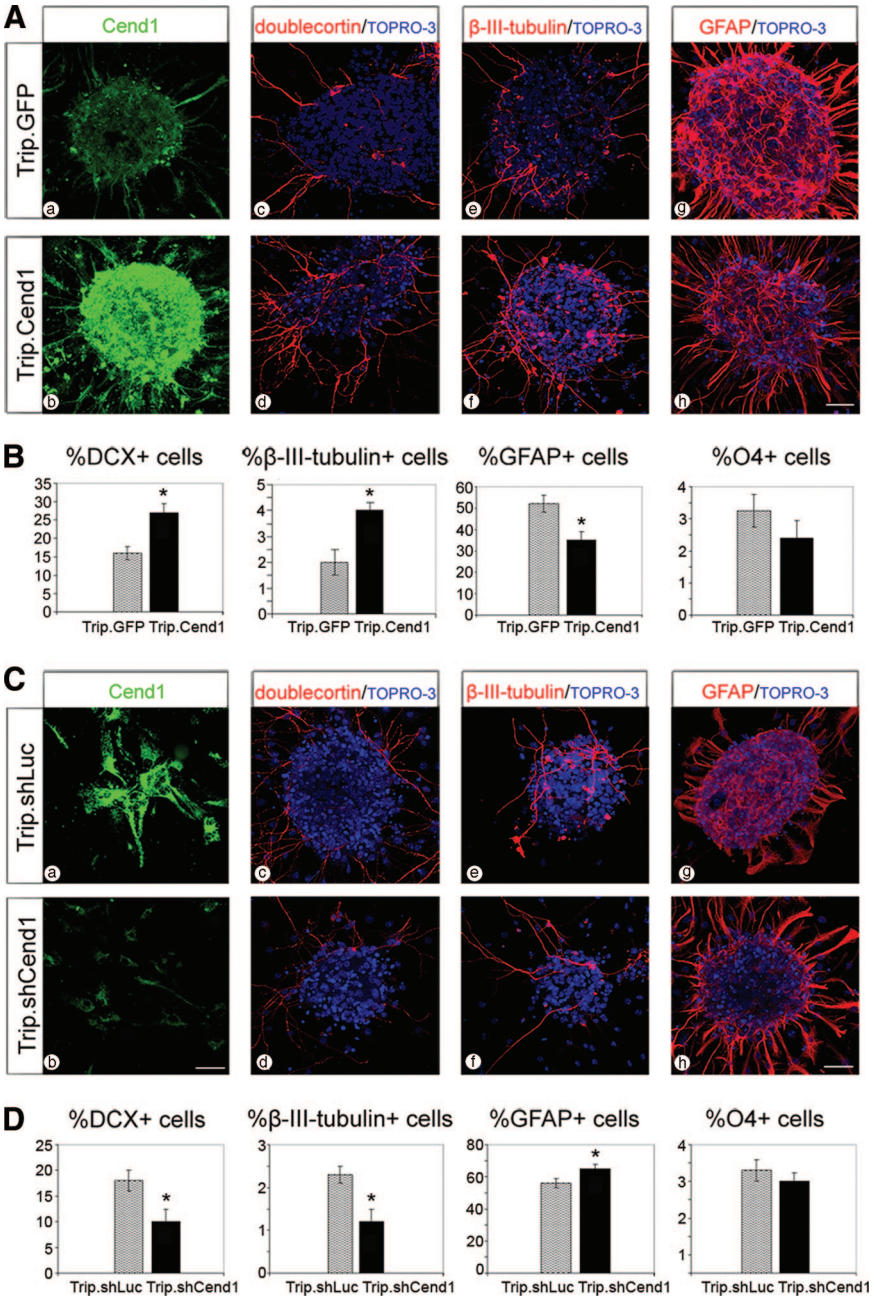

Figure 5. Qualitative and quantitative molecular phenotype analysis of neurosphere differentiation upon Cend1 overexpression and silencing. **(A):** Confocal images of differentiating neurospheres transduced with Trip.GFP or Trip.Cend1 and stained as whole-mount preparations for Cend1 (green), the indicated lineage (red), and TOPRO-3 (blue). Cend1 overexpression results in a qualitative increase of doublecortin$^+$ and βIII-tubulin$^+$ cells and a decrease of GFAP$^+$ cells. **(B):** Graphs presenting the quantitative phenotypic changes upon Cend1 overexpression. In dissociated neurospheres, the percentage of DCX and βIII-tubulin$^+$ cells is increased, whereas the percentage of GFAP$^+$ cells is decreased. *, $p < .05$ ($n = 4$). The difference in the percentage of O4$^+$ oligodendrocytes is not statistically significant. Measurements represent the percentage of lineage-marker$^+$ cells out of DAPI$^+$ nuclei in neurospheres dissociated to single cells and grown for 3 days in the absence of growth factors. **(C):** Confocal images of differentiating neurospheres transduced with Trip.shLuc or Trip-.shCend1 and stained as whole-mount preparations for Cend1 (green), the indicated lineage markers (red), and TOPRO-3 (blue). Cend1 knockdown enhances astrocytic differentiation and reduces the neuronal phenotype. **(D):** Graphs presenting the quantitative phenotypic changes upon Cend1 silencing. Neuronal markers (DCX and βIII-tubulin) decrease, GFAP$^+$ cells slightly increase, and O4$^+$ cells are not affected. Note the opposite effect of Cend1 silencing on neurosphere molecular phenotype, compared with that obtained in the overexpression experiments. Measurements were performed as in **(B)**. *, $p < .05$ ($n = 4$). Staining intensities for Cend1 are not comparable between the two control situations presented in **(A)** and **(C)**. Scale bars = 40 μm (**Cc, Cd, Ce, Cf, Cg, Ch**) and 20 μm (**Ca, Cb**). Abbreviations: DCX, doublecortin$^+$; GFAP, glial fibrillary acidic protein; GFP, green fluorescent protein; sh, short hairpin.

7B, 7C). In addition, the average chain length in Trip.Cend1-transduced explants was shorter by 21% ± 2% compared with wild-type or Trip.GFP-transduced explants (Fig. 7D). To try to distinguish whether reduced chain numbers are due to an effect on migration or proliferation, explants were given a 2-hour BrdU pulse before BrdU/Cend1 double immunofluorescence labeling (Fig. 7E). Quantification of BrdU$^+$ cells per explant revealed a statistically significant threefold decrease in the proliferation rate of explants in response to Cend1 overexpression compared with control explants (Fig. 7E, 7F). Conversely, a statistically significant 2.3-fold increase in BrdU incorporation was evident as a consequence of Cend1 silencing (Fig. 7E, 7G). Thus, in explants, as in neurosphere cultures, Cend1 expression levels interfere with cell proliferation, thus contributing to the number of cells generated and consequently the number of chains formed. However, a migration defect per se cannot be ruled out as, in addition to the antiproliferative effect, a reduction in chain length was also noted in response to Cend1 overexpression.

DISCUSSION

Adult neurogenesis is a complex phenomenon that requires the concerted action of numerous cell-intrinsic and extrinsic factors participating in mechanisms not yet fully understood. We present here, for the first time, evidence for a modulating role of Cend1 protein in this mechanism. Cend1 is expressed at low levels in type B and transit-amplifying type C progenitor cells of the adult SVZ, and its expression increases concomitantly with the degree of neuroblast maturation. To shed light on the functional significance of Cend1 upregulation upon transition of progenitor cells to neurons, we implemented lentiviral gene

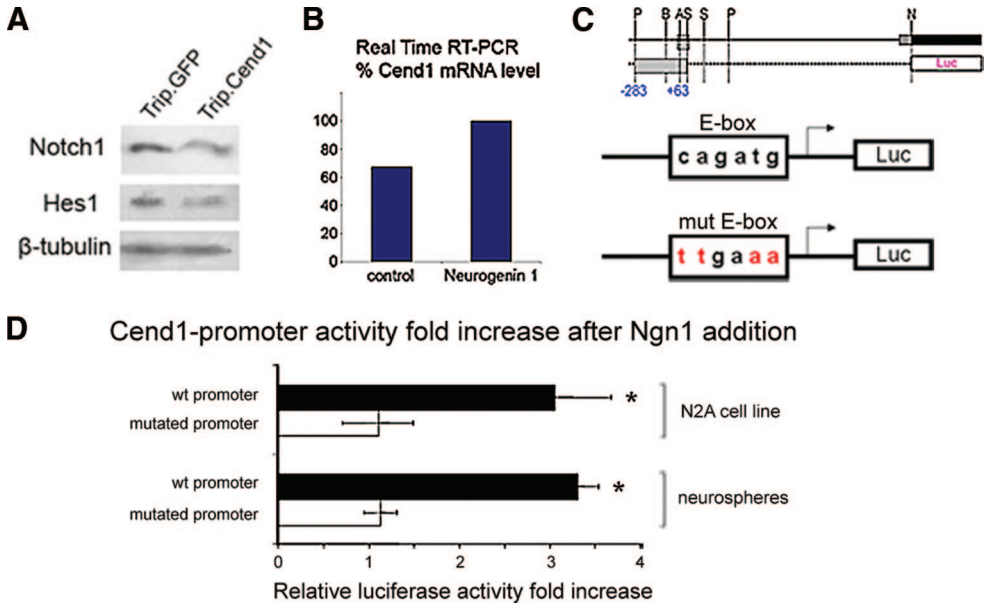

Figure 6. Cend1 participates in neuronal differentiation pathways. **(A):** Western blot analysis of neurospheres 4 days following transduction with the Trip.GFP and Trip.Cend1 lentiviral vectors reveals a 35% decrease of Notch1 and a 21% decrease of Hes1 protein levels upon Cend1 overexpression. **(B):** Real-time RT-PCR measurements of Cend1 mRNA in neurospheres transfected with the Neurogenin-1 (Ngn1) expression vector reveal a 35% increase in Cend1 mRNA levels. **(C):** Diagram illustrating the construct used for transactivation assays, in which a 346-base pair fragment of the human *Cend1* proximal promoter is linked to the Firefly Luciferase gene, as well as the four point mutations made in the **CA**G**A**T**G** E-box consensus sequence of the Cend1 promoter (−127/−132). **(D):** Measurement of Luciferase activity in Neuro 2a cells and neurospheres 2 days after cotransfection using the Ngn1 expression vector together with either the *Cend1* wt or E-box-mutated promoter constructs indicates a threefold increase of Cend1 promoter activity in the presence of Ngn1 compared with wt promoter only. This increase in Luciferase activity is reduced to basal levels when Ngn1 is cotransfected with the mutated E-box Cend1 promoter. *, $p < .05$ ($n = 3$). Abbreviations: A, AvaI; B, BamHI; GFP, green fluorescent protein; Luc, Luciferase; mut, mutated; N, NcoI; P, PstI; RT-PCR, reverse transcription-polymerase chain reaction; S, SmaI; wt, wild-type.

transfer technology to overexpress or downregulate Cend1 in vitro. The latter was accomplished by construction of highly efficient new-generation lentiviral vectors expressing a small hairpin RNA targeting Cend1 mRNA. The gain- and loss-of-function approaches resulted in a mirror effect, showing that Cend1 is involved in negatively regulating cell cycle progression and in promoting neuronal differentiation of neonatal precursors.

Cend1 Marks the Neurogenic Lineage of the Adult SVZ

The source of permanent cell production throughout life consists of NSCs known to belong to the astroglial lineage [5, 24], a finding that has changed the scenario concerning NSC origin and identity. Here, we asked whether Cend1, previously shown to characterize the neuronal lineage in the embryonic CNS from precursor to mature stage [8, 9], is also expressed by neuronal precursors in the adult SVZ, which is a much more complex area cyto-architecturally, containing a mixture of populations with different cycling properties, fate potential, and molecular phenotype [5]. Our data show that Cend1 is expressed by $GLAST^+$ and $GFAP^+$ astrocytes, a finding that comes in support of fate-mapping experiments proposing that the $GFAP^+$ NSCs of the adult SVZ originate from $GLAST^+$ embryonic radial glia [21, 25] and further phenotypically links these two populations. Besides its expression in type B precursors, in the SVZ Cend1 colocalizes with $Dlx2^+$ type C precursors [26] and $Pax6^+$ type A neuroblasts [8]. In addition, Cend1 levels rise in the OB, where it is highly expressed by $NeuN^+$ and $GABA^+$ interneurons. Taken together, these data indicate that Cend1 is present in neuronal progenitors and postmitotic neurons along the SVZ-RMS-OB pathway, thus marking the neuronal lineage in this region of the adult brain.

Cend1 Has a Dual Function Implicated in Cell Cycle Control and Differentiation of Neonatal SVZ-Derived NSCs

An intriguing observation is that Cend1 is present in precursor cells during the time window they generate neurons, whereas it is downregulated when they shift from a neurogenic to a gliogenic potential [8, 9]. Importantly, Cend1 expression is low in neuronal precursors and higher in differentiated neurons, implying that its expression levels may be critical for neuronal lineage progression. It is possible that this increase in Cend1 levels may function to measure proliferative time and eventually induce cell cycle withdrawal and/or elongation. Such a model for cell cycle control has been suggested by Durand and Raff [27]; this model involves the accumulation of the cell cycle inhibitor p27Kip1 in neural progenitors [27–29]. A similar model has recently been proposed for Notch1 to address its dual function in stem cell proliferation and differentiation [30]. To address whether this mechanism of action also applies to Cend1, we manipulated Cend1 expression in the neurosphere assay, by challenging Cend1 expression and following the cycling characteristics of progenitor cells, as well as their fate choice upon induction of differentiation. Our data indicate that Cend1 exerts a prominent antiproliferative effect, a finding further supported by the concomitant (but in the opposite direction) alteration in Cyclin D1 levels, which in each case paralleled the increased or decreased proliferation rates. The Cyclin D1 pathway is of major importance for cell cycle progression/exit in neuronal cells. It has been reported that upon neuronal differentiation, Cyclin D1 not only is downregulated but also becomes predominantly cytoplasmic as progenitor cells undergo cell cycle withdrawal and terminal differentiation [31]. Such a shift from nuclear to cytoplasmic Cyclin D1 localization, leading to activation of the p53-pRb pathway [32], was observed in neuroblastoma cells in response

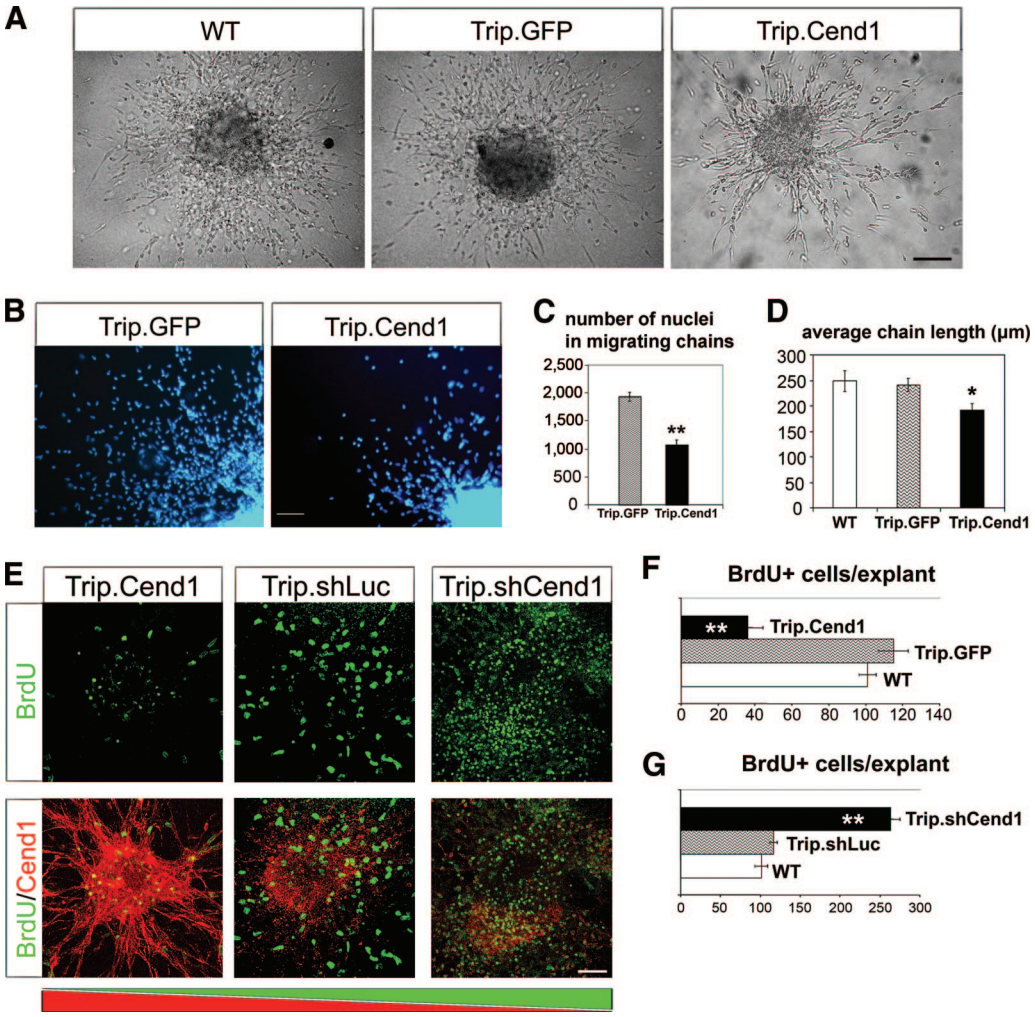

Figure 7. Effect of Cend1 overexpression and silencing on postnatal day 5 subventricular zone explants**. (A):** Phase-contrast images of WT and Trip.GFP-transduced explants exhibit similar morphology, whereas Trip.Cend1-transduced explants exhibit reduced number of migrating chains. **(B, C):** 4,6-Diamidino-2-phenylindole (DAPI) nuclear staining of control and Cend1-transduced explants **(B)** and quantification of $DAPI^+$ nuclei **(C)** indicate that the number of cells migrating outside the explant core is reduced in response to Cend1 overexpression. **, $p < .01$ ($n = 5$). **(D):** Estimation of the average chain length in WT, Trip.GFP-transduced, and Trip.Cend1-transduced explants reveals a statistically significant 21% ± 2% decrease in average chain length upon Cend1 overexpression. * $p < .05$ ($n = 4$). **(E):** Proliferation study following a 2-hour BrdU pulse in control (Trip.shLuc), Cend1-overexpressing (Trip.Cend1), and Cend1-silenced (Trip.shCend1) explants. Cend1 overexpression is correlated with a decrease in BrdU incorporation, whereas the opposite is observed upon Cend1 knockdown compared with the control situation. The Trip.GFP vector produced BrdU incorporation rates identical to those of the Trip.shLuc vector. **(F, G):** Graphs representing the changes in BrdU incorporation upon Cend1 overexpression **(F)** and downregulation **(G)**. **, $p < .01$ ($n = 5$). Scale bars = 40 μm **(A, B, F)**. Abbreviations: BrdU, 5-bromo-2′-deoxyuridine; GFP, green fluorescent protein; sh, short hairpin; WT, wild-type.

to Cend1 overexpression [12]. In addition, both gain- and loss-of function approaches in the neurosphere system, but also in vivo in the chick embryo early neural tube [13], imply that, apart from its antiproliferative function, Cend1 promotes neural stem/progenitor cell differentiation toward a neuronal phenotype. Taken together, our gain- and loss-of function data demonstrate that maintenance of low Cend1 expression contributes to a proliferative precursor state, whereas elevation of Cend1 expression participates in the mechanism controlling the precursor-to-postmitotic neuron transition.

Cend1 Forms Part of the NSC Differentiation Program During Neonatal Neurogenesis

Due to their extreme plasticity, adult SVZ NSCs attract particular attention for their potential use in cell replacement therapies of neurological disorders. The development of such approaches requires identification of the overlapping pathways of growth factors, neurotransmitters, transcription factors, and guidance molecules that regulate neurogenesis in the adult. To this end an increasing number of factors regulating this process have been identified. These include bFGF, brain-derived neurotrophic factor and ciliary neurotrophic factor (CNTF), which regulate NSC maintenance and self-renewal within the SVZ niche [33, 34], whereas Notch1, acting downstream of CNTF, controls NSC numbers [35]. Of relevance, our present data demonstrate downregulation of Notch1 and its downstream effector Hes1 [36] upon Cend1 overexpression. This downregulation is possibly due to the decreased number of progenitors produced in the total neurosphere population. However, it should be also mentioned that in vivo overexpression studies in the chick embryo spinal cord revealed that the subpopulation of neuronal progenitors overexpressing Cend1 downregulated Notch1 protein [13]. Similarly to Cend1, Numb/Numbl proteins are present in all types of SVZ precursors and have recently been shown to participate in

repair mechanisms of the subventricular niche [37]. Interestingly, the bHLH proneural protein Neurogenin-1, which has previously been shown to directly trans-activate *Cend1* promoter in the ND26 neuronal cell line [18], exerts the same activating effect on both Cend1 promoter and protein in the neurosphere system, indicating that Cend1 is part of the differentiation program activated by proneural genes. Importantly, alleviation of *Cend1* activation by Ngn1 upon mutation of the E-box consensus sequence present in the *Cend1* proximal promoter, constituting a putative bHLH protein binding site [38], indicates a direct action of Ngn1 on Cend1 transcription. Since proneural genes are transiently expressed in precursor cells and are readily downregulated in differentiated neurons, their ability to sustain neuronal differentiation relies on activation of downstream genes participating in cellular differentiation networks.

CONCLUSIONS

Our data demonstrate that Cend1 participates in neuronal differentiation networks controlled by proneural genes not only during embryonic but also during postnatal neurogenesis and that when its expression reaches above a threshold level it becomes crucial for the transition of neuronal precursors to differentiated neurons. Therefore, its use may have important implications for directing controlled differentiation of neural stem and precursor cells toward the neuronal lineage in cell replacement approaches using genetically modified endogenous or grafted precursor cells.

ACKNOWLEDGMENTS

This work was supported by Institut Pasteur Paris Grand Programme Horizontal on Stem Cells and the Hellenic General Secretariat for Research and Technology EPAN Grants YB-11 and YB-26. L.K. is the recipient of a doctorate bursary from Association France-Parkinson. P.-M.L. is also supported by the Fondation pour la Recherche Médicale, the Fédération pour la Recherche sur le Cerveau, the Agence Nationale de la Recherche (ANR-05-Neur-028-01), and the Fondation NRJ-Institut de France. We thank P. Souque for technical assistance and Dr. P. Politis for help with real-time RT-PCR assays. We also thank C. Dambly-Chaudière for useful comments on the manuscript and Drs. R. Kageyama and H. Ohkubo for providing us with reagents used in this study.

DISCLOSURE OF POTENTIAL CONFLICTS OF INTEREST

The authors indicate no potential conflicts of interest.

REFERENCES

1 Gage FH. Neurogenesis in the adult brain. J Neurosci 2002;22:612–613.
2 Menn B, Garcia-Verdugo JM, Yaschine C et al. Origin of oligodendrocytes in the subventricular zone of the adult brain. J Neurosci 2006;26:7907–7918.
3 Thored P, Arvidsson A, Cacci E et al. Persistent production of neurons from adult brain stem cells during recovery after stroke. STEM CELLS 2006;24:739–747.
4 Luskin MB, Parnavelas JG, Barfield JA. Neurons, astrocytes, and oligodendrocytes of the rat cerebral cortex originate from separate progenitor cells: An ultrastructural analysis of clonally related cells. J Neurosci 1993;13:1730–1750.
5 Doetsch F, Caille I, Lim DA et al. Subventricular zone astrocytes are neural stem cells in the adult mammalian brain. Cell 1999;97:703–716.
6 Mori T, Buffo A, Gotz M. The novel roles of glial cells revisited: The contribution of radial glia and astrocytes to neurogenesis. Curr Top Dev Biol 2005;69:67–99.
7 Ninkovic J, Gotz M. Signaling in adult neurogenesis: From stem cell niche to neuronal networks. Curr Opin Neurobiol 2007;17:338–344.
8 Koutmani Y, Hurel C, Patsavoudi E et al. BM88 is an early marker of proliferating precursor cells that will differentiate into the neuronal lineage. Eur J Neurosci 2004;20:2509–2523.
9 Politis PK, Rohrer H, Matsas R. Expression pattern of BM88 in the developing nervous system of the chick and mouse embryo. Gene Expr Patterns 2007;7:165–177.
10 Patsavoudi E, Merkouri E, Thomaidou D et al. Characterization and localization of the BM88 antigen in the developing and adult rat brain. J Neurosci Res 1995;40:506–518.
11 Mamalaki A, Boutou E, Hurel C et al. The BM88 antigen, a novel neuron-specific molecule, enhances the differentiation of mouse neuroblastoma cells. J Biol Chem 1995;270:14201–14208.
12 Gaitanou M, Buanne P, Pappa C et al. Cloning, expression and localization of human BM88 shows that it maps to chromosome 11p15.5, a region implicated in Beckwith-Wiedemann syndrome and tumorigenesis. Biochem J 2001;355:715–724.
13 Politis PK, Makri G, Thomaidou D et al. BM88/CEND1 coordinates cell cycle exit and differentiation of neuronal precursors. Proc Natl Acad Sci U S A 2007;104:17861–17866.
14 Zufferey R, Nagy D, Mandel RJ et al. Multiply attenuated lentiviral vector achieves efficient gene delivery in vivo. Nat Biotechnol 1997;15:871–875.
15 Ronca F, Yee KS, Yu VC. Retinoic acid confers resistance to p53-dependent apoptosis in SH-SY5Y neuroblastoma cells by modulating nuclear import of p53. J Biol Chem 1999;274:18128–18134.
16 Zennou V, Petit C, Guetard D et al. HIV-1 genome nuclear import is mediated by a central DNA flap. Cell 2000;101:173–185.
17 Gritti A, Frolichsthal-Schoeller P, Galli R et al. Epidermal and fibroblast growth factors behave as mitogenic regulators for a single multipotent stem cell-like population from the subventricular region of the adult mouse forebrain. J Neurosci 1999;19:3287–3297.
18 Papadodima O, Sergaki M, Hurel C et al. Characterization of the BM88 promoter and identification of an 88 bp fragment sufficient to drive neurone-specific expression. J Neurochem 2005;95:146–159.
19 Ohtsuka T, Asahi M, Matsuura N et al. Regulated expression of neurogenic basic helix-loop-helix transcription factors during differentiation of the immortalized neuronal progenitor cell line HC2S2 into neurons. Cell Tissue Res 1998;293:23–29.
20 Doetsch F, Garcia-Verdugo JM, Alvarez-Buylla A. Cellular composition and three-dimensional organization of the subventricular germinal zone in the adult mammalian brain. J Neurosci 1997;17:5046–5061.
21 Tramontin AD, Garcia-Verdugo JM, Lim DA et al. Postnatal development of radial glia and the ventricular zone (VZ): A continuum of the neural stem cell compartment. Cereb Cortex 2003;13:580–587.
22 Namba T, Mochizuki H, Onodera M et al. The fate of neural progenitor cells expressing astrocytic and radial glial markers in the postnatal rat dentate gyrus. Eur J Neurosci 2005;22:1928–1941.
23 McKay R. Stem cells in the central nervous system. Science 1997;276:66–71.
24 Seri B, Garcia-Verdugo JM, McEwen BS et al. Astrocytes give rise to new neurons in the adult mammalian hippocampus. J Neurosci 2001;21:7153–7160.
25 Merkle FT, Tramontin AD, Garcia-Verdugo JM et al. Radial glia give rise to adult neural stem cells in the subventricular zone. Proc Natl Acad Sci U S A 2004;101:17528–17532.
26 Aguirre AA, Chittajallu R, Belachew S et al. NG2-expressing cells in the subventricular zone are type C-like cells and contribute to interneuron generation in the postnatal hippocampus. J Cell Biol 2004;165:575–589.
27 Durand B, Raff M. A cell-intrinsic timer that operates during oligodendrocyte development. Bioessays 2000;22:64–71.
28 Ohnuma S, Harris WA. Neurogenesis and the cell cycle. Neuron 2003;40:199–208.
29 Gao FB, Durand B, Raff M. Oligodendrocyte precursor cells count time but not cell divisions before differentiation. Curr Biol 1997;7:152–155.
30 Guentchev M, McKay RD. Notch controls proliferation and differentiation of stem cells in a dose-dependent manner. Eur J Neurosci 2006;23:2289–2296.
31 Sumrejkanchanakij P, Tamamori-Adachi M, Matsunaga Y et al. Role of cyclin D1 cytoplasmic sequestration in the survival of postmitotic neurons. Oncogene 2003;22:8723–8730.
32 Weinberg RA. E2F and cell proliferation: A world turned upside down. Cell 1996;85:457–459.

33 Chojnacki A, Shimazaki T, Gregg C et al. Glycoprotein 130 signaling regulates Notch1 expression and activation in the self-renewal of mammalian forebrain neural stem cells. J Neurosci 2003;23:1730–1741.
34 Zheng W, Nowakowski RS, Vaccarino FM. Fibroblast growth factor 2 is required for maintaining the neural stem cell pool in the mouse brain subventricular zone. Dev Neurosci 2004;26:181–196.
35 Androutsellis-Theotokis A, Leker RR, Soldner F et al. Notch signalling regulates stem cell numbers in vitro and in vivo. Nature 2006; 442:823–826.
36 Kageyama R, Ohtsuka T, Hatakeyama J et al. Roles of bHLH genes in neural stem cell differentiation. Exp Cell Res 2005;306: 343–348.
37 Kuo CT, Mirzadeh Z, Soriano-Navarro M et al. Postnatal deletion of Numb/Numblike reveals repair and remodeling capacity in the subventricular neurogenic niche. Cell 2006;127:1253–1264.
38 Coulson JM, Fiskerstrand CE, Woll PJ et al. E-box motifs within the human vasopressin gene promoter contribute to a major enhancer in small-cell lung cancer. Biochem J 1999;344:961–970.


See www.StemCells.com for supplemental material available online.